

**ON MERIDIONAL STRUCTURE AND DYNAMICS OF THE
INTERTROPICAL CONVERGENCE ZONE**

A Thesis
Presented to
The Academic Faculty

by

Violeta E. Toma

In Partial Fulfillment
of the Requirements for the Degree
Master of Science in Earth and Atmospheric Sciences

Georgia Institute of Technology
August 2005

**ON MERIDIONAL STRUCTURE AND DYNAMICS OF THE
INTERTROPICAL CONVERGENCE ZONE**

Approved by:

Dr. Peter J. Webster, Advisor
School of Earth and Atmospheric Sciences
Georgia Institute of Technology

Dr. Judith A. Curry
School of Earth and Atmospheric Sciences
Georgia Institute of Technology

Dr. Robert X. Black
School of Earth and Atmospheric Sciences
Georgia Institute of Technology

Date Approved: July 13, 2005

*To the loving memory of my grandmother, Gherghina Bolan, whose teachings were more
valuable to me than any lessons.*

ACKNOWLEDGEMENTS

I am deeply appreciative of the valuable support from my advisor, Dr. Peter Webster. He provided guidance and strongly encouraged me to choose my own scientific path. I wish to thank Dr. Judith Curry and Dr. Robert Black for agreeing to take time out of their busy schedules, and for giving valuable suggestions and comments on this thesis.

I would like to thank the current and former members of my group - especially Dr. Hai-Ru Chang and Carlos Hoyos for their help and good suggestions.

I am thankful to my fellow students and good friends Arsineh Hecobian and Kelly Smolinski for their continued moral support.

I thank my parents for supporting my curiosity and letting me make my own mistakes and for their patience and love. Finally, my everlasting gratitude and love to my husband Ion, for his love, understanding, and enormous encouragement when it was most required.

TABLE OF CONTENTS

DEDICATION	iii
ACKNOWLEDGEMENTS	iv
LIST OF FIGURES	vi
SUMMARY	vii
I INTRODUCTION	1
II PHYSICAL PROCESSES THAT DETERMINE THE LOCATION OF THE ITCZ	7
III DATA AND METHODOLOGY	11
IV RESULTS	13
4.1 Vertical Structure of the Summer Meridional Circulation in the Tropical eastern Pacific Ocean	13
4.2 Vertical Structure of the Summer Meridional Circulation in the Atlantic Ocean	22
V CONCLUSIONS AND FURTHER DIRECTIONS	29
REFERENCE	32

LIST OF FIGURES

Figure 1	Zonally averaged circulation showing mass stream function ($10^{10} \text{ kg s}^{-1}$) for (a) March-May, (b) June-August, (c) September-November, (d) December-February	3
Figure 2	Vertical profiles of $gz + c_p T$ and $gz + c_p T + Lq$ in the equatorial trough. Then abscissa indicates the excess over $300 \text{ kJ} * \text{ kg}^{-1}$. Reproduced from Riehl and Malkus (1979)	4
Figure 3	Latitude-time description of Outgoing Longwave Radiation anomalies for (a) summer 1997, and (b) summer 1999; black line represents $\eta=0$ contour at 925mb level	14
Figure 4	Latitude- height profile of long time mean summer meridional circulation for the eastern Pacific Ocean (120W-90W)	16
Figure 5	Composite longitude-latitude plots of OLR anomalies (shaded contours) and the 850mb horizontal wind anomalies for (a) the disturbed, and (b) the undisturbed case	17
Figure 6	Latitude – height profile of meridional circulation averaged for three longitudinal bands in the eastern Pacifica ocean for (a), (b) disturbed case and (c), (d) undisturbed case	20
Figure 7	Composite of meridional wind at 925mb where $\eta=0$, relative humidity at 600mb level, OLR anomalies and cross-equatorial pressure difference for a region averaged between $120^\circ\text{W} - 110^\circ\text{W}$ and $10^\circ\text{N} - 15^\circ\text{N}$	23
Figure 8	(a) Longitude-latitude plot of OLR and 925mb horizontal wind; (b), (c) Latitude-height profile of long time mean summer meridional circulation for the Atlantic Ocean (35W-25W); (d) OLR, sea surface temperature (SST) and mean sea level pressure (MSLP)	24
Figure 9	Composite of meridional wind at 925mb where $\eta=0$, relative humidity at 600mb level, OLR anomalies and cross-equatorial pressure difference for a region averaged between $35^\circ\text{W}-25^\circ\text{W}$ and $5^\circ\text{N}-10^\circ\text{N}$	26
Figure 10	Composite latitude-height profile of meridional circulation averaged for $35^\circ\text{W}-25^\circ\text{W}$ longitudinal band at day -2 (a, c, e) and day 0 (b, d, f)	27

SUMMARY

The location of the Inter-Tropical Convergence Zone plays an important role in the climatology of tropical regions. Yet, despite its importance, the basic physics that determine the location of the ITCZ are not fully understood.

Observational analyses show that, where the cross-equatorial pressure gradient is strong, the maximum convection is not necessarily associated with the highest sea surface temperature (SST), or correspondingly, the lowest sea level pressure. Tomas and Webster (1997) argue that if a strong enough cross-equatorial pressure gradient exists and the system is inertially unstable, secondary ameliorating circulations will drive strong off-equatorial convection in regions where ITCZ location is determined by low tropospheric dynamics.

The observational record is re-examined to test the inertial instability hypothesis using the new ECMWF reanalysis data set. Composite analyses are performed to study the structure of the summer meridional circulation for the tropical Eastern Pacific Ocean and Atlantic Ocean.

In agreement with Tomas and Webster theory, we find that the magnitude of the cross-equatorial pressure difference appears to determine the intensity of convection with low values of outgoing longwave radiation always to the north of the $\eta=0$ line and the absolute vorticity advection equatorward of the $\eta=0$ line. Also the observed oscillation period of the disturbance for the studied regions coincides with theoretical oscillation period of the inertial flow.

CHAPTER I

INTRODUCTION

Understanding the Intertropical Convergence Zone (ITCZ) will help researchers improve tropical cyclogenesis forecasts and drought and flood predictions for the regions affected by tropical weather. There is no general theory to fully explain the location and strength of the ITCZ.

This paper focuses on understanding why the ITCZ is located away from the equator in some regions, the mechanism responsible for the intense off-equatorial convection, and the particular structure of the meridional circulation in those regions.

The tropical atmosphere is characterized primarily by high temperature values and abundant moisture content. The global energy balance between incoming solar radiation and outgoing long wave radiation illustrates a net heating at the equator and a net cooling at higher latitudes. Therefore, for equilibrium to exist there must be a net transport of energy by the atmosphere and ocean towards the poles, with warm moist air rising near the equator, moving poleward and descending at higher latitudes and then converging equator-ward near the surface. However, the Earth is rotating and the Coriolis force acts to change the direction of air motion. As a result, the winds in the upper troposphere become westerly and lower troposphere winds become easterly. This circulation is known as Hadley circulation. Edmond Halley first hypothesized this mechanism in 1686. He did not explain, however why the trade winds have an easterly direction. George Hadley (1735) explained that the cause of the easterly winds is due to the conservation of angular momentum on a rotating Earth. Usually the Hadley cell extends to about 30° on both

sides of the equator. Figure 1 shows zonally averaged mass stream functions for March-May (MAM), June-August (JJA), September-November (SON) and December-February (DJF) calculated by Webster (2004). It is important to notice that the Hadley circulation is not symmetrical about the equator. Except for MAM and slightly into summer, the Hadley circulation reduces to one cell with intensified upward motion near the equator and downward motion over the winter hemisphere. The observed Hadley circulation is highly dependent on moisture content.

The effect of moisture is to create asymmetry between ascent and descent. In moist convection the upward motion covers a smaller area than the downward motion, with the strength of the updrafts much stronger than the strength of the downdrafts.

Riehl and Malkus (1958, 1979) were the first to identify the role of the tropical depression as an important source of heat for the atmosphere. They recognized that the trade wind circulation could not explain the lateral energy transport towards the poles. Trades in fact, act to export energy towards the equator. The transfer of heat must be accomplished by the export of potential energy poleward. They noticed that the upward calculated energy flux could not be due to the mean flow, because the observed profile of moist static energy has a minimum at mid levels. The observed profile of dry static energy is increasing almost linearly through the troposphere until the tropopause, remaining statically stable (Figure 2). They introduced the concept of the “hot tower mechanism” of undiluted cumulonimbus in the ITCZ. This mechanism was invoked to carry energy from the surface layer through the mid troposphere energy minima into the upper troposphere, where it would be exported laterally to higher latitudes.

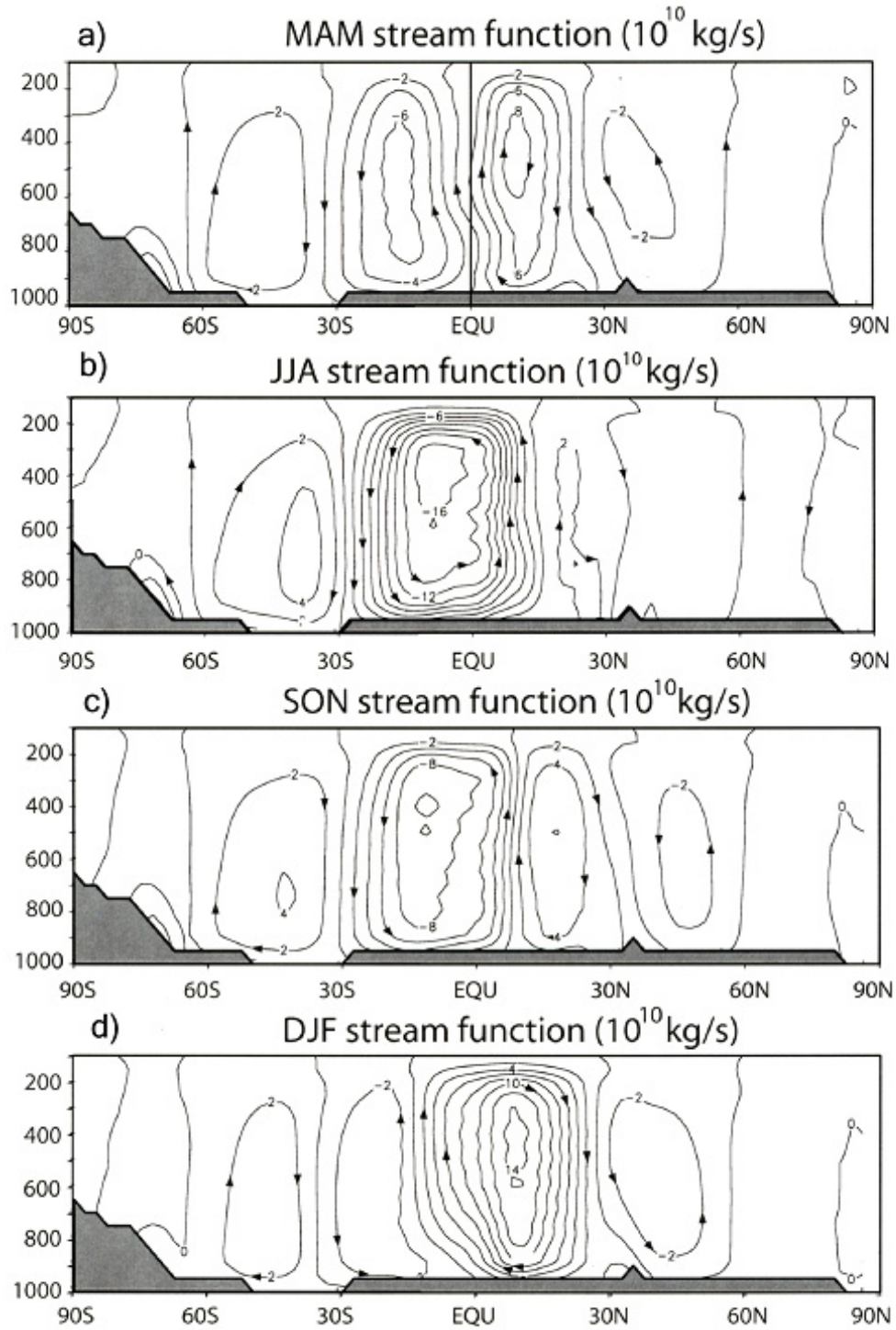


Figure 1 Zonally averaged circulation showing mass stream function (10^{10} kg s⁻¹) for (a) March-May, (b) June-August, (c) September- November, (d) December-February. The stream functions represent the average flow in the latitude-height plane. Reproduced with permission from Webster (2004).

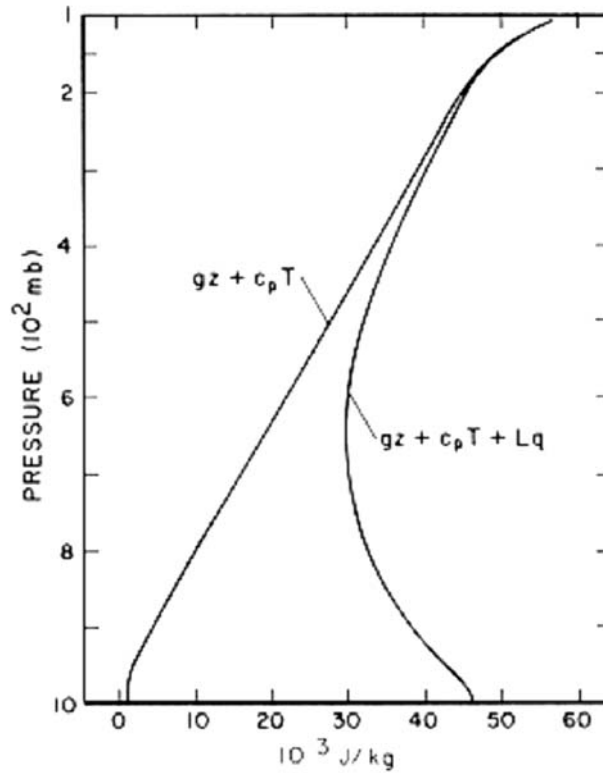


Figure 2 Vertical profiles of $gz + c_p T$ and $gz + c_p T + Lq$ in the equatorial trough. Then abscissa indicates the excess over $300 \text{ kJ} \cdot \text{kg}^{-1}$. Reproduced from Riehl and Malkus (1979).

Riehl and Malkus concluded that approximately 1600-2400 hot towers with average area of 125 km^2 and ascent speed of 2-3 m/s are needed to meet the heat balance evolved in their paper. Observations over the tropical oceans suggest that there is no evidence of “undiluted updraft cores” and the updraft velocities are smaller than those consistent with adiabatic lifting. Zipser (2003) found that the reversible liquid water content within the cloud needed for the adiabatic ascent postulated by Riehl and Malkus is three orders of magnitude larger than the observed one, probably due to large dilution by entrainment. Riehl and Malkus realized the importance of moisture in the deep

convection mechanism, but their theory is not in accord with observations and we need to find alternative explanations.

Observations show that ITCZ stays north of the equator over the Atlantic and Eastern Pacific Ocean with enhanced convection at latitudes of about 4° to 10° relative to the equator, although the annual-mean solar radiation at the top of the atmosphere is symmetric with respect to the equator. Emanuel (1994) argued that fluctuations in the subcloud-layer thickness are related to fluctuations in boundary layer entropy. While very different from the “hot towers mechanism”, Emanuel’s approach underlines the importance of moist static energy in deep convection. The large-scale flow developed in his paper is determined by the low-level temperature and humidity and wind profile. Charney and Eliassen (1964) argued that the interaction between small-scale cumulus cells and hurricane formation leads to large-scale conditional instability of the second kind (CISK). Charney (1971) argued that the location of the ITCZ is due to a balance between Ekman pumping and moisture availability (as a result of maximum sea surface temperature). However, in the case of the Eastern Pacific Ocean the warmest waters are along the continental coast, and not over the region with maximum precipitation. Lindzen and Nigam (1987) underlined the importance of sea surface temperature (SST) difference in the determination of the ITCZ convection. They argued that convective anomalies are always determined by SST gradient and convection takes place over the regions where the SST is maximum. To a first approximation, rising motion, minimum sea level pressure (SLP), minimum outgoing longwave radiation (OLR), and maximum SST should be collocated. Analysis of several observational datasets (Hastenrath 1991, Waliser and Somerville 1994, Tomas and Webster 1997) show that, even though

increased values of SST are necessary for the ITCZ to occur, maximum convection is not always co-located with maximum SST values.

Held and Hou (1980) tried to predict the strength and the width of this circulation using a zonally symmetric model with maximum heating located at the equator. The model makes use of angular momentum conservation and thermal wind balance. Although the Held-Hou model provides a reasonable estimate of poleward extension (22,000 km) of the Hadley circulation, it gives a very poor estimate of the strength of the circulation. The calculated meridional wind is 0.5 cm s^{-1} . However, observed meridional winds at the tropics are closer to 1 m/s. Lindzen and Hou (1988) extended the Held-Hou model for the case of asymmetric heating, centered off the equator but at the same time retaining the other assumptions described above. Their results were closer to the observations, with a much stronger simulated meridional circulation. When the maximum heating is over the summer hemisphere, the winter cell becomes stronger and moves towards the summer hemisphere and the summer cell becomes very weak as is seen in Figure 1. While the above mechanism incorporates basic dynamics with angular momentum conservation and thermal wind balance, it does not explain why the heating is centered off the equator and it does not include the effect of latent heating and cooling and assumes a dry atmosphere.

Numerous modeling studies have tried to reproduce the ITCZ (e. g Hess, Battisti and Rasch 1993, Numaguti 1993, Ferreira and Schubert 1997). While these experiments have produced diverse results, the responsible mechanism for ITCZ formation remains to be clarified and is still under intense debate.

CHAPTER II

PHYSICAL PROCESSES THAT DETERMINE THE LOCATION OF THE ITCZ

Angular momentum conservation and thermal wind balance arguments provide a good qualitative understanding of the zonally average tropical circulation but fail to explain the observed strength and structure of ITCZ. While based on different mechanisms, most of the aforementioned theories work under the assumption that the upper level deep-convection plays a minor part in the forcing of low-level convergence. They assume that the low-level convergence is responsible for the location and intensity of the deep convection. Held-Hou and Lindzen-Hou experiments showed that for the same magnitude of the external heating the atmospheric response varies significantly with latitude. This must be due to the rotational effect. But what is the forcing that determines deep convection to develop in regions where the atmosphere is statically stable?

The present study investigates the mechanism responsible for the intense off-equatorial convection, and attempts to explain the observed profile of the meridional circulation over those regions. Tomas and Webster, 1997 and Zhang et al., 2004 presented evidence of mid-tropospheric southward divergent wind in the monthly mean meridional circulation for the eastern Pacific Ocean. Tomas and Webster argued that in regions where the cross-equatorial pressure gradient is strong, the flow is inertially unstable, and the maximum convection is not necessarily associated with highest SST; SST should be large but not necessarily a maximum (differing from Lindzen and Nigam

assumptions, but in agreement with the observations). They argued that strong off-equatorial convection is determined more by lower tropospheric dynamics than by lower boundary temperature. Tomas, Holton and Webster (1999) conducted a series of experiments, using a two-dimensional boundary layer model to test the Tomas and Webster theory. However, their hypothesis was tested on diagnostic analysis over a short time period, thus further research to clarify this is necessary.

A short physical and mathematical description of inertial instability, ignoring non-linear, frictional and diabatic effects is presented. This basic derivation can offer a good qualitative understanding of the underlying physics. In determining the potential for inertial instability we follow Holton (1992), Tomas and Webster (1997) and Knox (2003) using the parcel method and assume that the basic flow is entirely zonal (only along the x-axis). In this case, we have $v_g = 0$. Assuming the flow is purely geostrophic, the equations of motions are:

$$\frac{D_H u}{Dt} - f v_{ag} = 0 \quad (1)$$

$$\frac{D_H v_{ag}}{Dt} = f(u_g - u) \quad (2)$$

where D_H/Dt is the total horizontal derivative, v_{ag} is the meridional ageostrophic wind, f is the Coriolis parameter and $u = u_g + u_{ag}$. Combining equations (1) and (2):

$$\frac{D_H^2 v_{ag}}{Dt^2} + [f(f + \zeta_g)] v_{ag} = 0$$

where $\zeta_g = -\partial u_g / \partial y$ is the geostrophic relative vorticity. The above equation looks similar to the static stability equation. If we assume a wave solution for v_{ag} as an exponential

function of time, $v_{ag} = Ae^{i\sigma^2 t}$, where $\sigma = [f(f + \zeta_g)]^{1/2}$ is the oscillation frequency, we have three distinct cases:

a) inertially stable atmosphere for $f(f + \zeta_g) > 0$, with oscillation period $\frac{2\pi}{[f(f + \zeta_g)]^{1/2}}$,

b) inertial neutrality for $f(f + \zeta_g) = 0$,

c) inertial instability for $f(f + \zeta_g) < 0$, with e-folding time $\frac{1}{[-f(f + \zeta_g)]^{1/2}}$

From the above equations we notice that inertial instability is not restricted to any particular region, but is expected to appear where the Coriolis parameter is very small, i.e. the tropics. At least two processes are particular at the equator. First, the Coriolis parameter vanishes and then changes sign across the equator. For the Northern Hemisphere the inertial instability condition becomes $f < \partial u_g / \partial y$. Consequently, a strong cross-equatorial pressure gradient, and a large wind shear may lead to inertially unstable flow. Regionally, the Eastern Pacific, Indian and Atlantic Oceans, display strong equatorial pressure gradients, providing possible conditions for inertial instability. Furthermore, the inertial instability condition for the Northern Hemisphere can be written as $\eta_g < 0$, where $\eta_g = f + \zeta_g$ represents the geostrophic absolute vorticity.

The inertial instability condition requires that a parcel be displaced poleward from its equilibrium position to accelerate in the direction of the displacement. Thus the wind will accelerate equatorward of the $\eta = 0$ contour and will slow down to the poleward side of the $\eta = 0$ contour, for the Northern Hemisphere during summer. In regions where the wind accelerates, divergence should appear, and regions where the wind decreases should

become convergent. Holton defines the oscillation period of the inertial flow as $\frac{2\pi}{|f|}$. At

6°N, inertial period becomes ≈ 4.5 days. There is a 4.5-day oscillation in the location of zero absolute vorticity contours and rain anomalies in the eastern Pacific Ocean, presented in the following chapters.

CHAPTER III

DATA AND METHODOLOGY

To understand the ITCZ, we completed a detailed diagnostic using numerical weather prediction reanalysis products and satellite based products for the period 1981-2000. Zonal and meridional wind, specific humidity, and air temperature data for 18 vertical levels (1000, 925, 850, 775, 700, 600, 500, 400, 300, 250, 200, 150, 100, 70, 50, 30, 20, 10) with horizontal resolution of one degree and daily temporal resolution were used. SST, mean sea level pressure (MSLP) and orographic data with horizontal resolution of 2.5 degrees and daily temporal resolution were used. These products were provided by the European Center for Medium-Range Weather Forecasts (ECMWF) ERA-40 Years Re-analysis from their website <http://data.ecmwf.int/>. As a proxy for precipitation, OLR daily data with 2.5-degree by 2.5-degree horizontal resolution were used. Daily OLR data were provided by the NOAA-CIRES Climate Diagnostics Center, from their Web site at <http://www.cdc.noaa.gov>. Absolute vorticity and horizontal wind divergence fields were numerically derived using the central difference approximation following Holton's (1992) definitions. Relative humidity at each grid point was calculated following Curry and Webster (1999).

The mass stream functions that describe the mean meridional circulation (MMC) were evaluated following Hartmann's (1994) formula:

$$\Psi_M = \frac{2\pi a \cos \varphi}{g} \int_o^p [v] dp ,$$

where a represents the radius of the Earth, φ latitude, g gravitational acceleration, $[v]$ zonal mean meridional wind, and p pressure.

The composite results presented in this study are for the eastern Pacific Ocean and Atlantic Ocean. These two specific tropical oceanic regions were chosen because they are characterized by strong off-equatorial ITCZ.

CHAPTER IV

RESULTS

4.1 Vertical Structure of the Summer Meridional Circulation in the Tropical eastern Pacific Ocean

Analysis of the time series of eastern Pacific OLR and absolute vorticity at 925mb were performed for several years. In all studied cases the results were very similar. The low level $\eta = 0$ contour oscillates between equator and 2-8°N, with an approximate period of 4-5 day. Figure 3 represents two examples of temporal evolution of convective precipitation for the eastern Pacific Ocean during JJA season. In comparison with a normal year, for year 1997 (El Nino) the convective band seems to be broader and generally slightly closer to the equator and there is larger variability in OLR values. The ITCZ is to the south of its normal position. In the year 1999 (La Nina) the precipitation band is farther away from the equator. However, we note that there is a 4.5-day oscillation of the location of zero absolute vorticity contours and that the disturbance is moving towards E – NE. Thus, the calculated theoretical temporal scale of the inertial oscillation coincides with the observed scale. The convective region is always positioned to the north of $\eta = 0$ and minimum OLR anomalies seem to appear when $\eta = 0$ contour reaches its northern point.

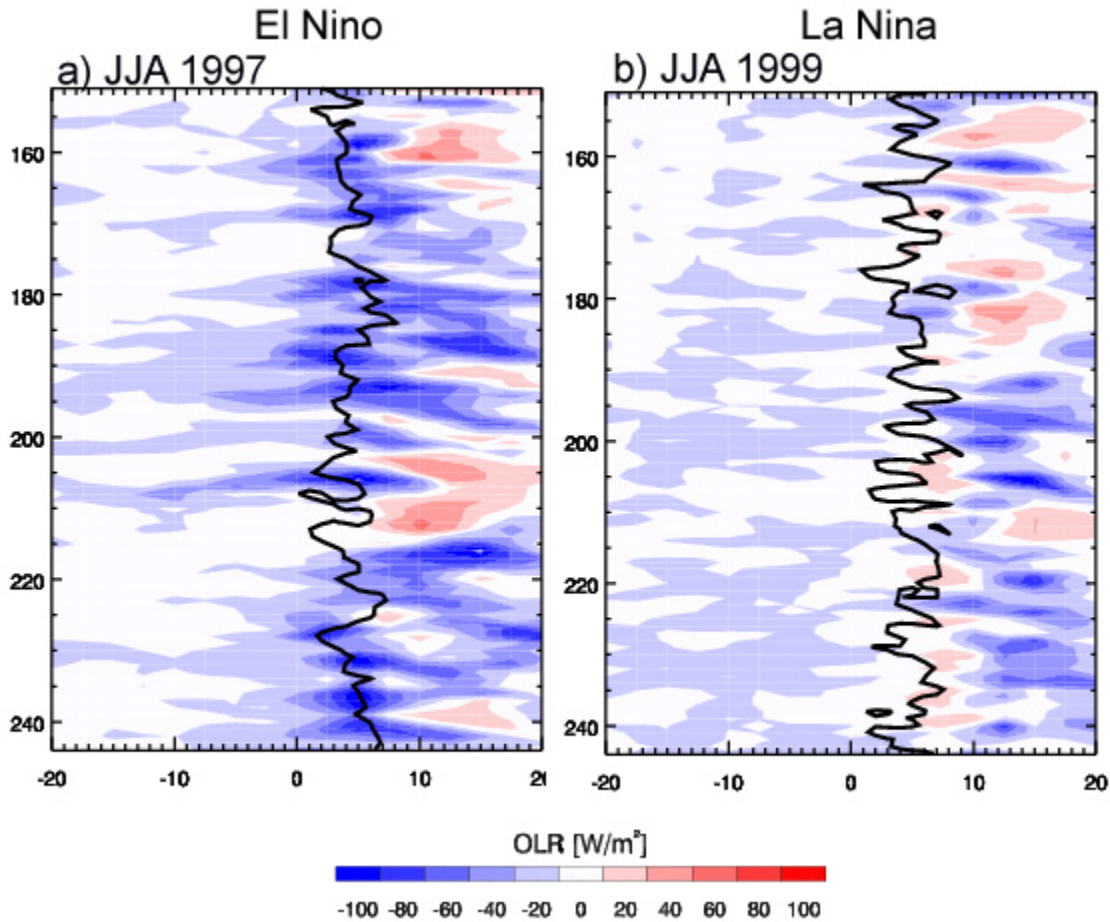


Figure 3 Latitude-time description of OLR anomalies for (a) summer 1997, and (b) summer 1999; the black line represents $\eta=0$ contour at 925mb level. Plotted data represent daily values for the 120°W-110°W longitudinal sector.

Zonally averaged circulation for the eastern Pacific Ocean (120°W-90°W) for JJA (Figure 4) indicates the presence of a cross-equatorial pressure gradient and large-scale deep convection, characterized by strong low-level convergence at about 8-10°N and corresponding upper tropospheric divergence. The resultant average JJA meridional wind is northward at lower levels with the maximum co-located with zero absolute vorticity line, southward at upper levels, and a somewhat weaker northerly flow in the middle troposphere. The corresponding zonally averaged mass stream functions for JJA, for the

120°W-90°W show the average upward flow to the north of the equator confined in a narrow band over the low level convergent region and the downward flow extended between equator and 20°S. The humidity profile shows high values of relative humidity over the ascending region and very dry atmosphere over the descending region. Thus, for the eastern Pacific Ocean case (Figure 4a) lower level convergence away from equator appears at about 10°-12°N to the north of the $\eta = 0$ contour. At 200 mb the $\eta = 0$ contour is situated to the south of the Equator, with positive advection of absolute vorticity due to reversed flow. This suggests that there are conditions for inertial instability in the upper troposphere as well.

SST maximum is situated to the north of the maximum low level convergence (co-located with the minimum OLR values). Tomas and Webster explained the observed mean meridional circulation and the relative location of the maximum SST, minimum OLR and minimum SLP for this region in terms of inertial instability. Tomas and Webster hypothesized that, in regions where the location of zero absolute vorticity contours is away from the equator, the system is inertially unstable. The deep large-scale cross-equatorial circulation advects negative absolute vorticity across the equator. In order to reduce the instability, generation of cyclonic absolute vorticity will take place by “vortex tube stretching” (in agreement with potential vorticity conservation). This will produce forced upward motion. If the atmosphere is conditionally unstable and a parcel has enough moisture when it reaches the level of free convection, it becomes positively buoyant. Thus, deep convection will develop, regardless of the moist static energy profile calculated by Riehl and Malkus. Additionally, we argue that the pattern apparent in Figure 4 is the result of the combined effects of two distinct types of circulation: deep

convective circulation and shallow dry circulation. The mid-tropospheric northerly flow apparent in the mean flow is the result of a dry circulation (more shallow equivalent depth, due to the lack of significant condensational heating).

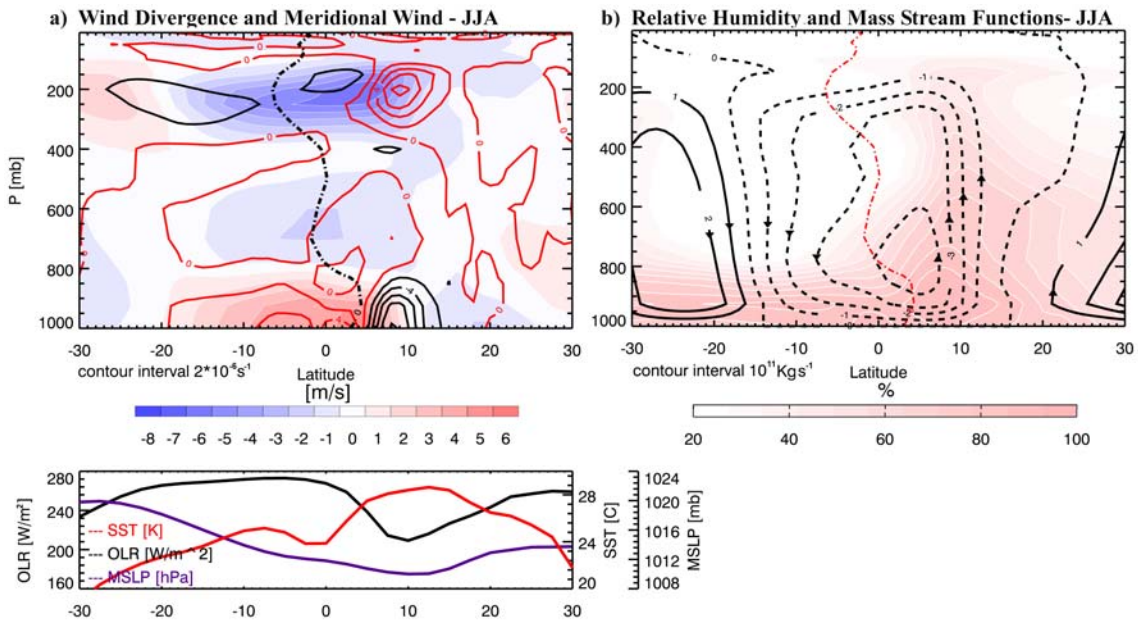


Figure 4 Latitude- height profile of long time mean summer meridional circulation for the eastern Pacific Ocean (120W-90W). (a) Wind divergence (red contours – positive values, black contours – negative values) and meridional wind (shaded contours); (b) relative humidity (shaded contours) and mass stream functions (solid lines- positive values, dashed line – negative values); (c) OLR (blue line), SST (red line), mean SLP (black line). The dash-dotted line represents $\eta=0$ contour.

We try to isolate the effect of moisture on the meridional circulation mechanism by examining two distinct cases. We focused our attention on the 120°W - 110°W longitudinal band and selected 52 days with strong negative OLR anomalies (usually associated with precipitation) and 51 days with strong positive OLR anomalies (associated with lack of precipitation). All days for composite were selected from the JJA season, when the eastern Pacific ITCZ is located entirely over the Northern Hemisphere.

Figure 5 shows the composite OLR anomalies, horizontal wind anomalies and $\eta=0$ contour for the 850mb level. For the disturbed case the minimum OLR anomalies are located between 8°N and 16°N and the corresponding horizontal wind vector anomalies cyclonically rotate into the disturbance, with maximum northward displacement of the zero absolute vorticity line. For the undisturbed case the OLR anomalies have maximum values between 7.5°N and 15°N with wind anomalies directed toward W-SW, and with zero absolute vorticity line located closer to the equator. Also, there appears to be significant anomalies in the horizontal winds over the Central American continent, with anomalous northeasterly 850mb horizontal wind for the disturbed case and anomalous southwesterly 850mb horizontal wind for the undisturbed case.

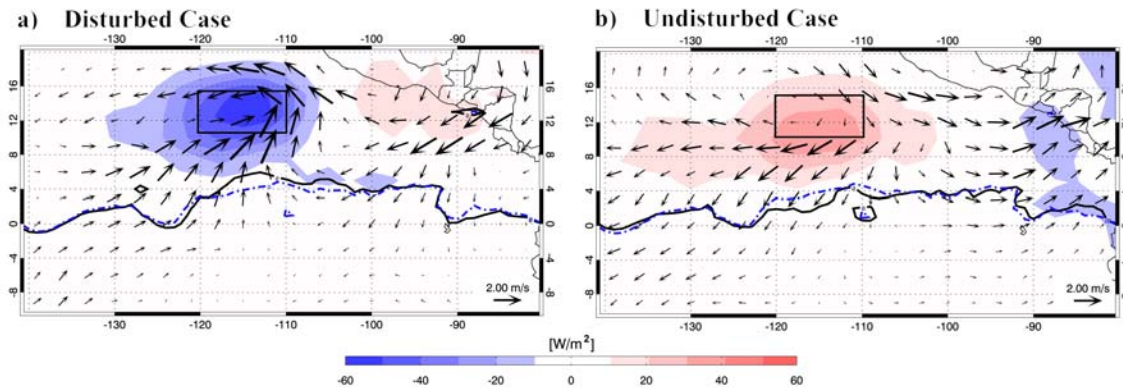


Figure 5 Composite longitude-latitude plots of OLR anomalies (shaded contours) and the 850mb horizontal wind anomalies for (a) the disturbed case, and (b) the undisturbed case. The solid black line represents $\eta=0$ contour for the 850mb level. The blue dash-dotted line represents $\eta=0$ contour for the 850mb level, averaged for JJA.

Figure 6 presents a complete picture of these two cases. Latitude–height profiles for three distinct longitudinal bands ((i) 135°W – 130°W , (ii) 120°W – 110°W , (iii) 95°W – 90°W) were plotted. For the disturbed case the meridional flow, over the maximum convergent area (120°W – 110°W) is composed of deep intense circulation with strong

mass convergence and southerly meridional wind at the lower level, over the region of minimum OLR anomalies, and strong divergence and northerly meridional wind at upper levels. The corresponding relative humidity field shows increased moisture in the middle and upper troposphere, over the low level convergent region. The mass stream functions complete the deep circulation picture, with upward mass transport over the convergent region and downward mass transport, on the equator side of this region. In order to have a complete picture of the developments of convection for this region we extended the analysis away from the center of the disturbance. The meridional profile averaged for the 95W-90W longitudinal band and for 135W-130W longitudinal band display the characteristics of dry circulation, being similar to the undisturbed case, suggesting that the except during the development of convection this seems to be the state of meridional circulation over this region. In the undisturbed case meridional circulation appears to be shallow with northerly meridional wind in the middle troposphere over the low level convergent region. We also notice the presence of a much weaker northerly meridional wind at upper level.

It is a matter of further research to investigate whether the apparent upper level pattern is due to mass conservation constraints or is due to intricacies involved in choosing the right days for composites. However, is clear that the deep large-scale (Hadley – like) pattern dominates the disturbed (highly convective) case, and in the undisturbed (dry) case the meridional circulation is confined to the middle and lower troposphere. Furthermore, in this last case, in contrast to the disturbed case, the middle troposphere is very dry. Another s difference between the disturbed and the undisturbed case appears in the upper level meridional wind at midlatitudes, in the Southern

Hemisphere. In the undisturbed case there is increased northward wind with maximum at about 200 mb with the mass stream functions suggesting strong subsidence at 15°S – 25°S. In the disturbed case the meridional wind at midlatitudes, in the Southern Hemisphere is northerly almost throughout the entire troposphere. The location of the zero absolute vorticity line at low levels is closer to the equator in the undisturbed case, and displaced northward in the disturbed case. These two cases above are characteristic for two distinct modes of the meridional circulation in the tropical regions, the deep convective mode that includes the effect of moisture, and the shallow dry mode.

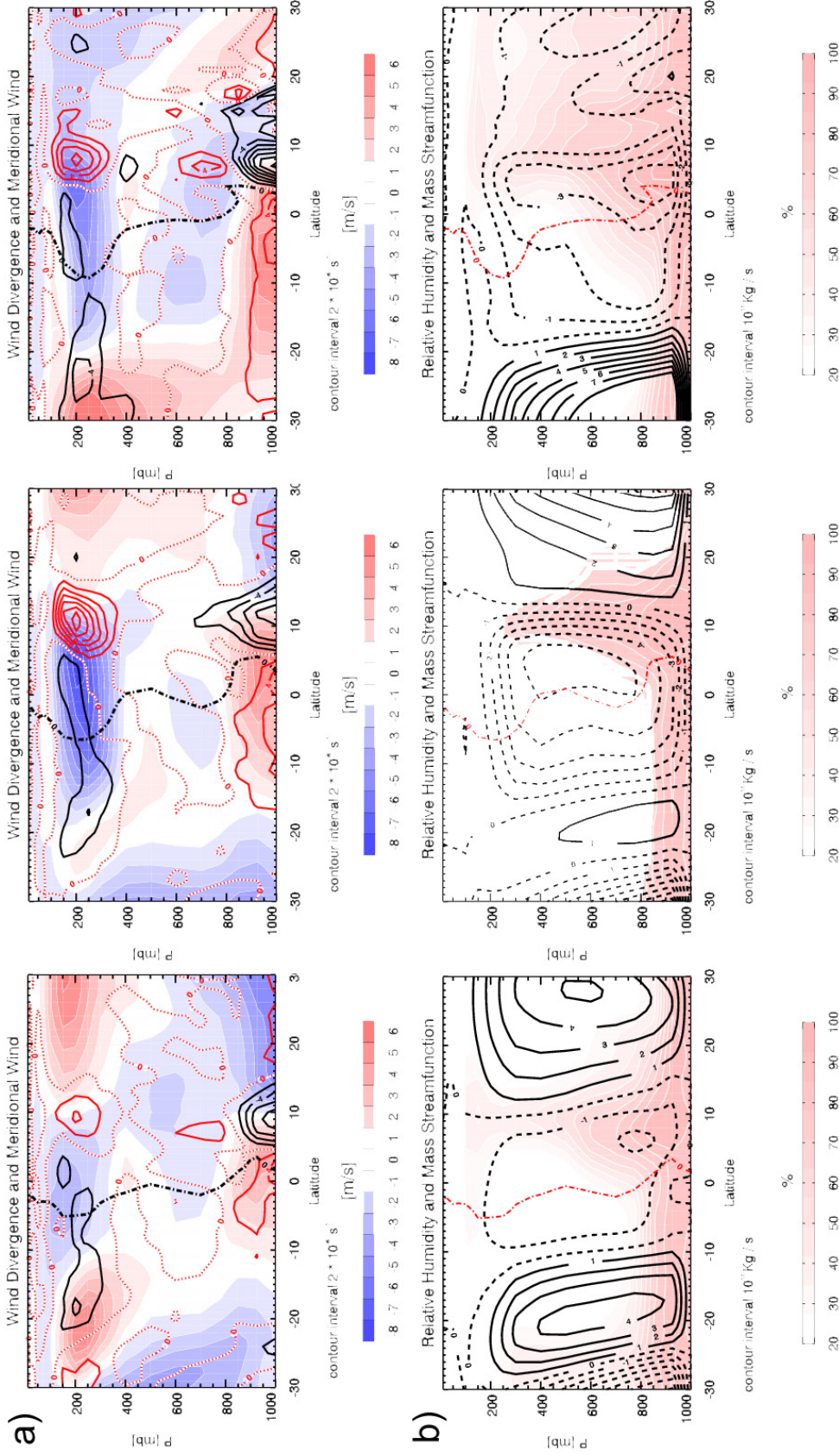


Figure 6 Latitude – height profile of meridional circulation averaged for three longitudinal bands in the eastern Pacific ocean for (a) (b) disturbed case and (c), (d) undisturbed case: (a), (c) wind divergence (red contours – positive values, black contours- negative values) and meridional wind (shaded contours); (b), (d) relative humidity (shaded contours) and mass stream functions (solid lines- positive values, dashed line – negative values) The dash-dotted line represents $\eta=0$ contour. Plotted data is averaged for the (i) 135°W -130°W, (ii) 120°W – 110°W, (iii) 95°W -90°W longitudinal bands.

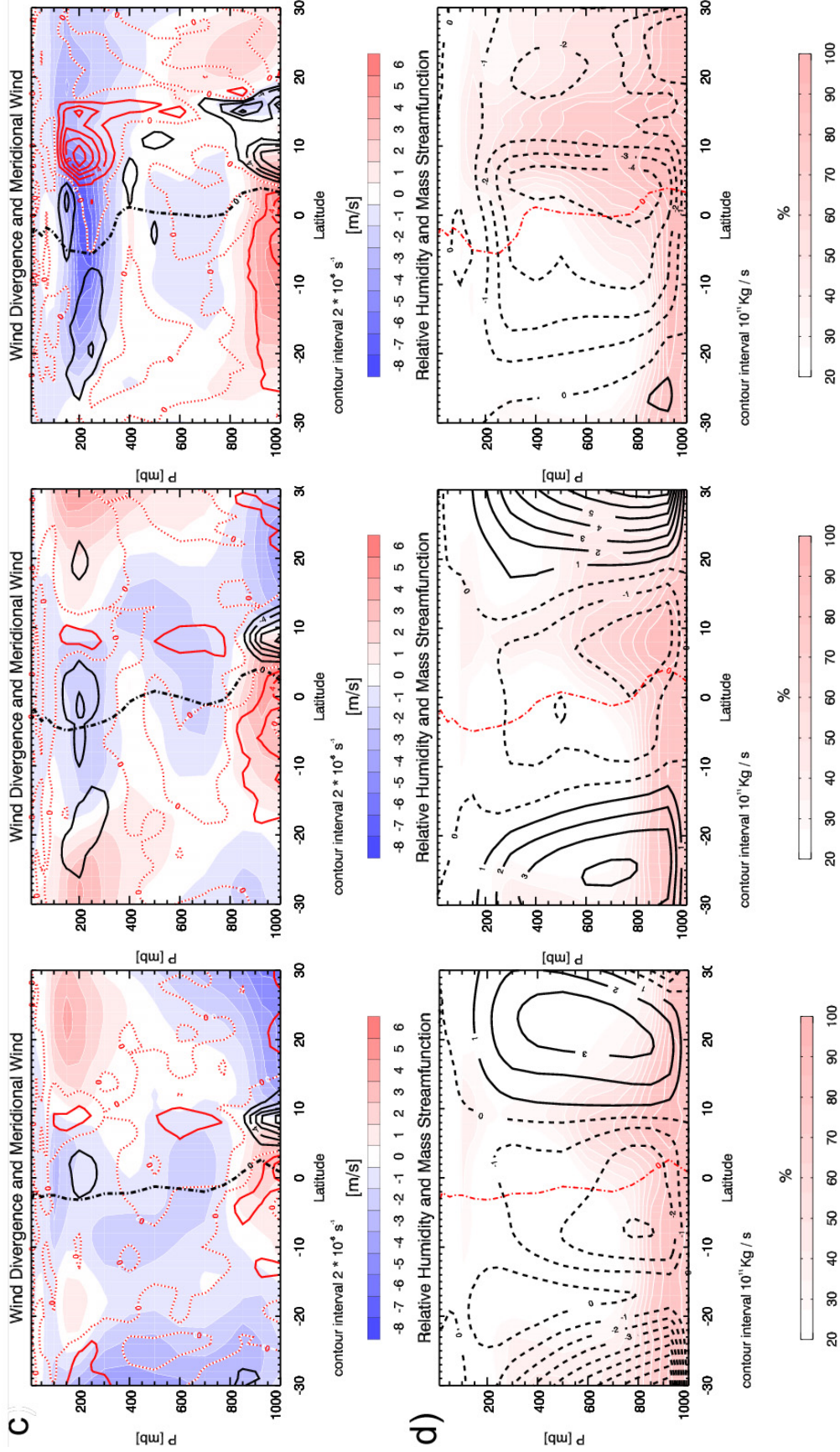


Figure 6 (cont)

Figure 7 shows composite values of meridional wind at 925 mb at $\eta=0$, relative humidity at 600 mb level, OLR anomalies and the cross-equatorial pressure difference (for a region averaged between 120°W - 110°W and 10°N - 15°N, marked by the black rectangle in figure 5 (a, b)). The criterion for choosing the composite is the same, with day 0 representing the composite result of the 52 days with strong negative OLR anomalies. The cross-equatorial pressure difference is calculated as the difference between mean SLP at 10°N and mean SLP at 10°S. The time of minimum OLR associated with increased precipitation is indicated as day 0. We note that minimum values in cross-equatorial pressure difference precede minimum OLR. This supports our hypothesis that the large-scale pressure gradient determines the intensity and location of maximum convection away from the equator. As expected, larger values of mid-tropospheric RH follow minimum values of OLR anomalies. We notice a 5 days oscillation period for the meridional wind at 925 mb and OLR anomalies, with minimum OLR coinciding with maximum southerly wind.

4.2 Vertical Structure of the Summer Meridional Circulation in the Atlantic Ocean

The analysis was extended to the Atlantic ITCZ in an effort to understand the major differences between the development of convective precipitation over the two tropical oceanic regions. Figure 8 shows that the band with minimum OLR (increased tropical precipitation) is centered at about 7.5 N over the central and western Atlantic and at about 10N over the eastern Atlantic Ocean and is much wider over the West Africa continent.

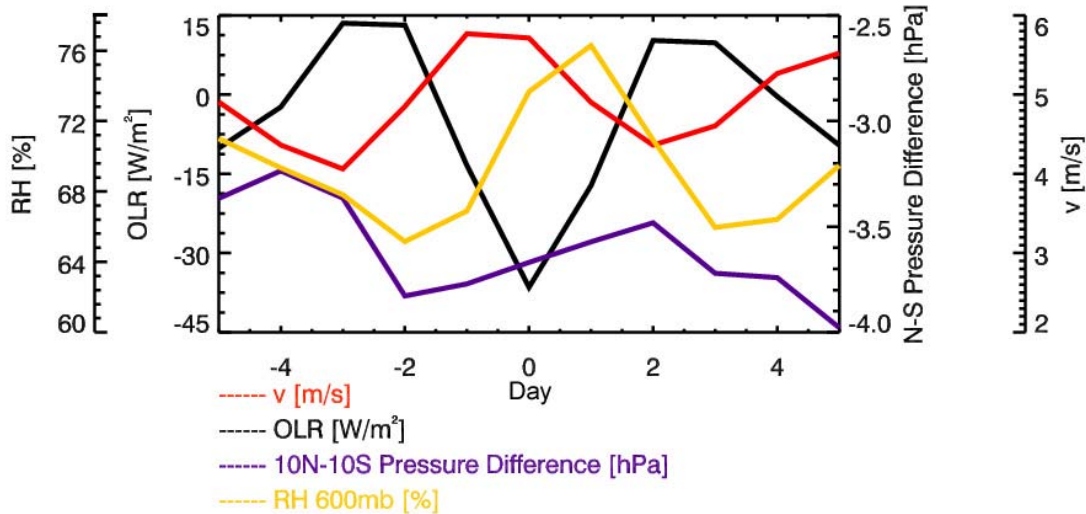


Figure 7 Composite of meridional wind at 925 mb where $\eta=0$, relative humidity at 600 mb level, OLR anomalies and cross-equatorial pressure difference for a region averaged between $120^{\circ}\text{W} - 110^{\circ}\text{W}$ and $10^{\circ}\text{N} - 15^{\circ}\text{N}$. The time of minimum OLR is indicated as day 0. The cross-equatorial pressure difference is calculated as the difference between mean SLP at 10°N and mean SLP at 10°S .

The 925 mb horizontal wind pattern shows the presence of cross-equatorial flow with the $\eta=0$ line to the north of the equator. It is evident that increased SST values are important to the formation of convection.

Unlike the eastern Pacific Ocean, in this case the temperature gradient is much smaller for this region and maximum SST is located slightly to the south of maximum convergence. The summer mean vertical profile is calculated for a longitudinal band west of the African continent at $35^{\circ}\text{W}-25^{\circ}\text{W}$, where we assume a reduced effect from the land surface processes. The meridional wind over the convergent region is southerly from the surface to about 750 mb and it becomes northerly with a maximum at the 250 mb level.

The mass stream-functions show a weaker mass transport to the Southern Hemisphere than seen in the Eastern Pacific case. It is well known that African easterly waves are important for the rainfall over tropical Atlantic and West Africa during JJA season.

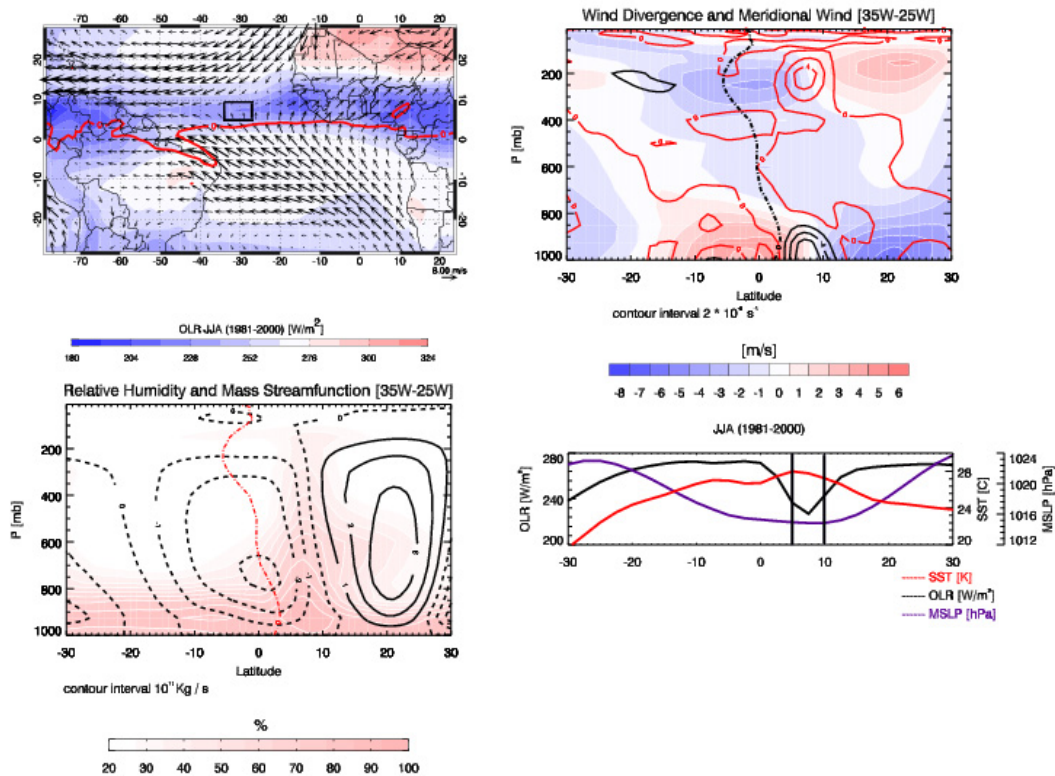


Figure 8 (a) Longitude –latitude plot of OLR (shaded contours) and 925 mb horizontal wind. Latitude – height profile of long time mean summer meridional circulation for the Atlantic Ocean (35W-25W); (b) wind divergence (red contours – positive values, black contours – negative values) and meridional wind (shaded contours); (c) relative humidity (shaded contours) and mass stream functions (solid lines- positive values, dashed line – negative values); (d) OLR (blue line), SST (red line), mean SLP (black line). The dash-dotted line represents $\eta=0$ contour

They are characterized by 3 to 5 day period and the average wavelength of the disturbance is about 2500-3000 km (e.g. Carlson 1969, Holton, 1992). Despite its significance, the nature of this disturbance and the way it interacts with convection is still

not clear. Future work plans to extend the present analysis to try to understand the impact of inertial instability in the development of this disturbance.

We choose 49 summer days with significant negative OLR anomalies for the 35°W-25°W; 10°N-5°N Atlantic Ocean region, marked by the black rectangle in figure 8 a). In figure 9 (similar to figure 7), the composite fields of meridional wind at 925 mb at $\eta=0$, relative humidity at 600 mb level, OLR anomalies and cross-equatorial pressure for the above region are shown.

The time of minimum OLR, associated with increased precipitation is indicated as day 0. Similar to the Eastern Pacific case, minimum values in cross-equatorial pressure difference precede minimum OLR. However for this region the cross-equatorial pressure gradient is much smaller than for the Eastern Pacific.

Maximum southerly meridional wind at 925 mb coincides with minimum OLR. Relative humidity values for 600 mb level, at day zero are smaller for the Atlantic case than for the Eastern Pacific suggesting a dryer mid-troposphere for the latter.

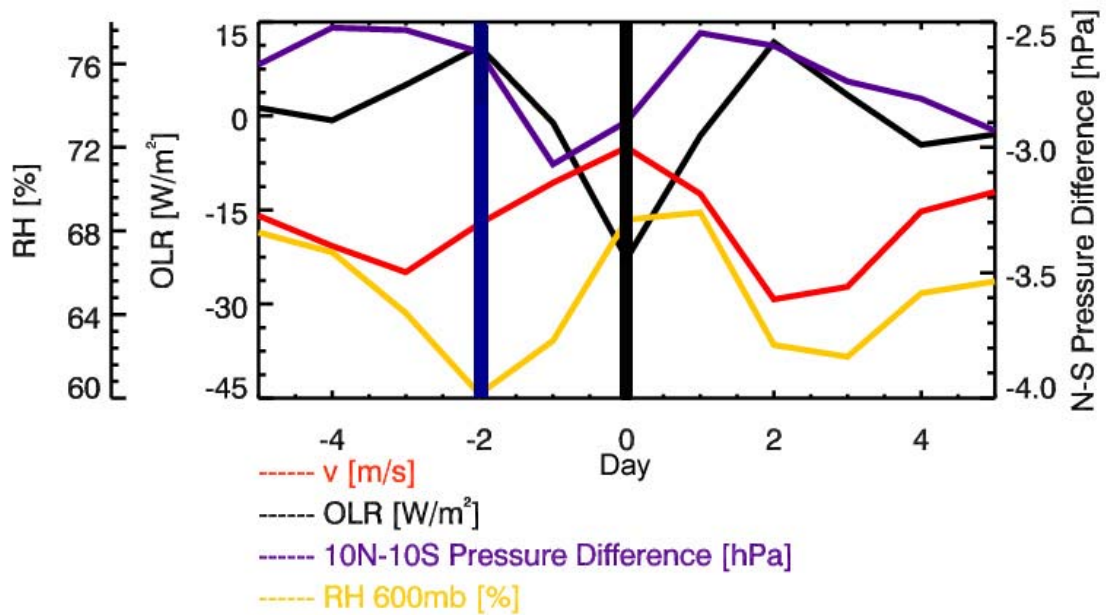


Figure 9 Composite of meridional wind at 925 mb where $\eta=0$, relative humidity at 600 mb level, OLR anomalies and cross-equatorial pressure difference for a region averaged between $35^{\circ}\text{W} - 25^{\circ}\text{W}$ and $5^{\circ}\text{N} - 10^{\circ}\text{N}$. The time of minimum OLR is indicated as day 0. The cross-equatorial pressure difference is calculated as the difference between mean SLP at 10°N and mean SLP at 10°S .

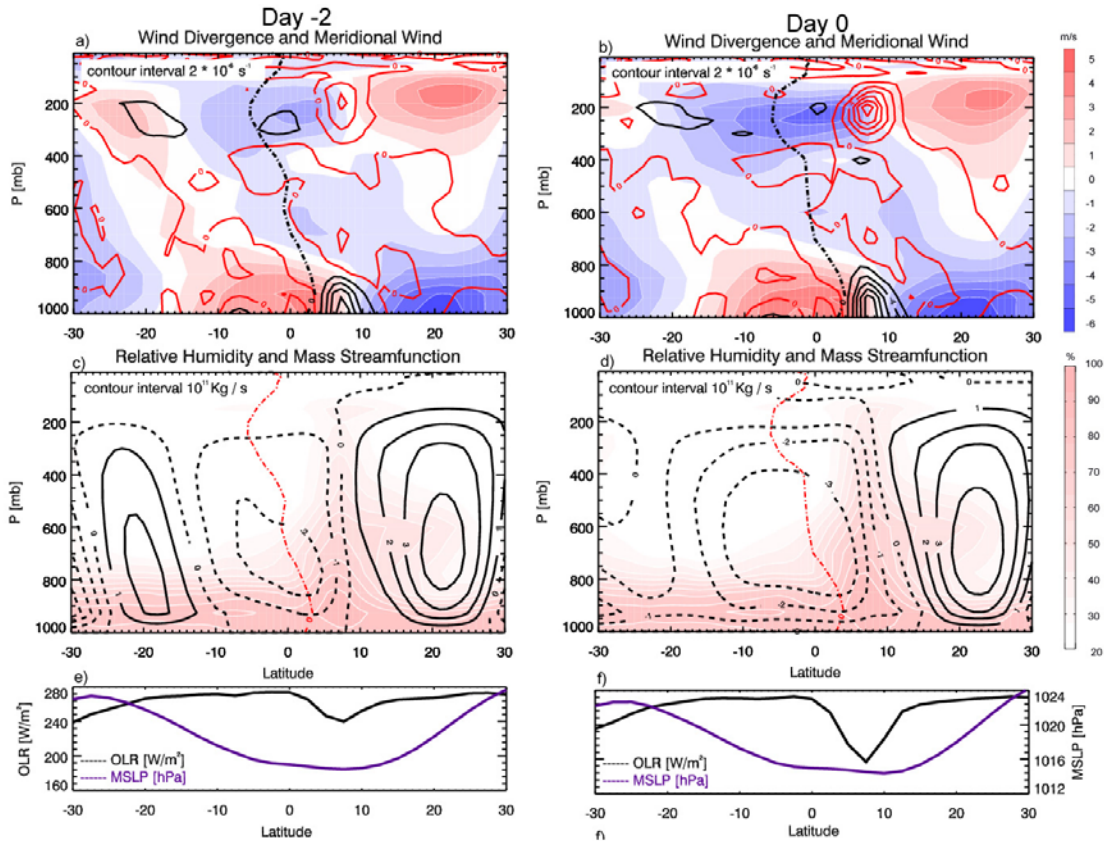


Figure 10 Composite latitude – height profile of meridional circulation averaged for 35°W-25°W longitudinal band at day –2 (a, c, e) and day 0 (b, d, f). (a), (b) wind divergence (red contours – positive values, black contours- negative values) and meridional wind (shaded contours); (c), (d) relative humidity (shaded contours) and mass stream functions (solid lines- positive values, dashed line – negative values) The dash-dotted line represents $\eta=0$ contour. (e), (f) OLR (black line), mean SLP (blue line).

The latitude – height profiles at day -2 (positive OLR anomalies), and day 0 (largest negative OLR anomalies) were plotted in Figure 10. There is no considerable difference between the mean sea level pressure gradient profiles for the two days, even though cross-equatorial pressure gradients exist for both cases. At day –2, the meridional circulation appears to be shallow with northerly meridional wind in the mid-troposphere over the low-level convergent region and weaker northerly meridional wind at upper levels. For day 0 (larger negative OLR anomalies) the meridional flow shows strong mass

convergence and southerly meridional wind at lower levels, over the region of minimum OLR anomalies (with the convergent region, centered at about 7°N closer to the equator than in the Eastern Pacific case), and strong divergence and northerly meridional wind at upper levels.

The relative humidity field shows increased moisture in the middle and upper troposphere, over the low level convergent region. There is weaker southward mass transport in the Atlantic region compared to the Pacific region. The difference between the disturbed and the undisturbed case appears in the upper level meridional wind in the southern midlatitudes, for this case as well. In the undisturbed case southerly wind is maximum at about 250 mb. The two cases above represent two modes of the meridional circulation in the tropical regions: the deep convective mode that includes the effect of moisture, and the shallow dry mode.

CHAPTER V

CONCLUSIONS AND FURTHER DIRECTIONS

Composite analyses of 20-yr ECMWF reanalysis data set were done to examine the structure of the ITCZ for the eastern Pacific Ocean and Atlantic Ocean and to investigate if the ITCZ convection away from equator can be explained in terms of inertial instability. These regions were chosen because the maximum sea surface heating is not at the same latitude as the minimum OLR, the maximum ITCZ rainfall is away from the equator, and stays in the Northern Hemisphere even though the annual-mean solar radiation at the top of the atmosphere is symmetric with respect to the equator. For both cases lower level convergence appears at about 5° - 12° N, north of the $\eta = 0$ contour. At 200mb the $\eta = 0$ contour is situated to the south of the Equator, with positive advection of absolute vorticity due to reversed flow. This suggests that there are conditions for inertial instability in the upper troposphere as well. In agreement with Tomas and Webster hypothesis, $\eta = 0$ contour at 925 mb has an approximate oscillation period of 4-5 day.

The maximum SST is similar for the two oceans (about 28° C) generating comparable moisture availability. However, the SST gradient is much larger for the eastern Pacific (Figures 4c and 8d), resulting in larger cross-equatorial pressure gradient and greater potential for instability. Thus, there is more intense rainfall and larger meridional mass transport for the eastern Pacific (Figures 6b (ii) and 10d). In contrast to McGauley, M., C. Zhang, and N.A. Bond, (2004), we have shown that the mean observed

meridional circulation for the studied regions, with the presence of a reverse meridional wind in the mid-troposphere, is the result of summing two modes of the meridional circulation in the tropical regions, the deep convective mode that includes the effect of moisture, and the shallow dry mode. In interpreting the results presented in this paper it must be remembered that the data used were reanalysis products and OLR variability was the only criterion in choosing the days for composite.

Tomas et al. (1999) consider the role inertial instability on lower level flow using a two-dimensional boundary model. When they assumed a non-linear solution for the basic state pressure field, resulting in a nonlinear geostrophic wind, their model reproduced the low level convergence well. They only considered boundary layer dynamics. We intend to extend the investigation and evaluate whether large-scale circulation will develop using MM5 modeling system that includes detailed dynamics, microphysics and cloud physics parameterizations schemes. Further experiments will be done to quantify the direct effect of the humidity, since our current theoretical approach assumes a dry atmosphere.

The atmospheric response to a prescribed pressure and temperature fields using different cloud parameterization schemes will be tested. The consequences of cross-equatorial advection of potential vorticity, which occurs when the cross-equatorial pressure gradient is sufficiently large, will be examined in detail. We will analyze the large-scale response by varying the SST and SST gradient, influencing the strength of the cross equatorial flow. We will also investigate the effect of moisture on the large-scale circulation. Further experiments will be run in which the same magnitude SST is placed at the equator.

Finally, given the similarity between the time scales of easterly waves and inertial period oscillation we will test the hypothesis to see whether the relaxation of instability is important in the generation of easterly waves in the tropical system.

REFERENCE

- Arakawa, A., and W. H. Schubert, 1974: Interaction of a cumulus cloud ensemble with the large-scale environment. Part I. *J. Atmos. Sci.*, **31**, 674-701.
- Battisti D.S., Sarachik E.S., and Hirst A.C., 1999: A consistent model for the large-scale steady surface atmospheric circulation in the tropics. *J. Climate*, **12**, 2956-2964.
- Carlson, T. N., 1969: Synoptic histories of three African disturbances that developed into Atlantic hurricanes. *Mon. Wea. Rev.*, **97**, 256–276.
- Charney, J. G, 1971: Tropical cyclogenesis and the formation of the Intertropical convergence zone. *Lectures in Applied Math.*, **13**, 355-368.
- Charney, J. G. and A. Eliassen, 1964: On the growth of the hurricane depression. *J. Atmos. Sci.*, **21**, 68-75.
- Curry, J. A. and Webster, P. J, 1999: Thermodynamics of Atmospheres and Oceans, *Academic Press*.
- Emanuel, K.A., 1995: On thermally direct circulations in moist atmospheres. *J. Atmos. Sci.*, **52**, 1529-1534.
- Ferreira, R. N., and W. H. Schubert, 1997: Barotropic aspects of ITCZ breakdown. *J. Atmos. Sci.*, **54**, 261-285.
- Hartmann, D. L., 1994: Global Physical Climatology, *Academic Press*.
- Held, I. M., and Hou, A. Y., 1980: Nonlinear axially symmetric circulations in a nearly inviscid atmosphere. *J. Atmos. Sci.* **37**, 515-533.
- Hess, P.G., D.S. Battisti and P. Rasch, 1993: "Maintenance of the Intertropical Convergence Zones and the Large-Scale Tropical Circulation on a Water Covered Earth." *J. Atmos. Sci.*, **50**, 691-713.
- Holton, J. R., 1992: An Introduction to Dynamic Meteorology, Third Edition. *Academic Press*.
- Knox, J.A., 2002: Inertial Instability, *Encyclopedia of Atmospheric Sciences*, 1004-1012.
- Lindzen, R. S., and S. Nigam, 1987: On the role of sea surface temperature gradients in forcing low-level winds and convergence in the Tropics. *J. Atmos. Sci.*, **44**, 2418–2436.

- Lindzen, R. S., and Hou A. Y., 1988: Hadley circulations for zonally averaged heating centered off the equator. *J. Atmos. Sci.* **45**, 2416-2427.
- McGauley, M., Zhang C., and Bond N. A., 2004: Large-scale characteristics of the atmospheric boundary layer in the eastern Pacific cold tongue/ITCZ region. *J. Climate*, **17**, 3907-3920.
- Numaguti, A., 1993: Dynamics and Energy Balance of the Hadley Circulation and the Tropical Precipitation Zones: Significance of the Distribution of Evaporation. *J Atmos. Sci.*, **50**, 1874-1887.
- Riehl, H., and J. S. Malkus, 1958: On the heat balance in the equatorial trough zone. *Geophysica*, **6**, 503-537.
- Riehl, and J. (Malkus) Simpson, 1979: The heat balance in the equatorial trough zone, revisited. *Contrib. Atmos. Phys.*, **52**, 287- 305.
- Tomas, R. A., J. R. Holton, and P. J. Webster, 1999: The influence of cross-equatorial pressure gradients on the location of near-equatorial convection. *Quart. J. Roy. Meteor. Soc.*, **125**, 1107-1127.
- Tomas, R. and P. J. Webster, 1997: On the location of the Intertropical convergence zone and near-equatorial convection: The role of inertial instability. *Quar. J. Roy. Met. Soc.*, **123**, 1445-1482.
- Waliser, D. E., and R. C. J. Somerville, 1994: Preferred latitudes of the Intertropical Convergence Zone. *J. Atmos. Sci.*, **51**, 1619-1639.
- Webster, P. J., 2004: The elementary Hadley circulation, *submitted*.
- Zhang, C., M. McGauley, and N.A. Bond, 2004: Shallow meridional circulation in the tropical eastern Pacific *J. Climate*, **17**, 133-139.
- Zipser, E. J., 2003: Some views On “Hot Towers” after 50 years of tropical field programs and two years of TRMM data. *Meteorological Monographs*: Vol. **29**, No. 51, 49-58.